Impact of Chuck Boundary Conditions on Wideband On-Wafer Measurements

Gia Ngoc Phung
Physikalisch-Technische Bundesanstalt
Bundesallee 100
38116 Braunschweig, Germany
gia.phung@ptb.de

Uwe Arz
Physikalisch-Technische Bundesanstalt
Bundesallee 100
38116 Braunschweig, Germany
uwe.arz@ptb.de

***Abstract*—While a lot of investigations have been presented recently explaining the parasitic effects in on-wafer measurements caused by probes, neighborhood and environmental effects, this paper addresses the impact of chuck boundary conditions. Starting from a coplanar waveguide (CPW) measurement example, this paper demonstrates how the most relevant chuck parameters, i.e. thickness and relative permittivity, deteriorate the S-parameters of CPWs.**

***Index Terms*—coplanar waveguides, leakage, radiation, surface waves**

I. Introduction

On-wafer measurements have been known as ambitious and challenging especially at higher frequencies because of different parasitic effects caused by the probes, by crosstalk with neighboring structures, and by multimode propagation and radiation effects. Recently, the influence of probes in interaction with the neighborhood in the layout [1], crosstalk behavior between adjacent structures [2] and multimode propagation e.g. due to surface waves [3], [4], [5] have been thoroughly investigated in the framework of the PlanarCal project [6]. As a result, a guideline [7] for the suppression of these effects has been proposed. One major finding was that the quality especially of coplanar waveguide (CPW) measurements is not only affected by the parasitics described above but also strongly depends on the measurement boundary conditions presented by the chuck material employed.

This guide [7] proposes that one should use a material for the chuck with a similar or higher permittivity than that of the substrate containing the devices to be tested in order to mitigate the propagation of surface waves. However, the investigations leading to [7] were based on simulations which assume that the measurement is performed on a ceramic chuck extending to infinity. In real measurements, the DUTs are normally situated on a substrate placed over a ceramic chuck support with finite thickness with a large metal chuck below, as shown in the measurement setup of Fig. 1. Therefore, an open question is whether the recommendations of the guide [7] still hold for the multi-layered measurement stackup of Fig. 1 and how the chuck parameters affect the S-parameters of measured DUTs. As a starting point, the measurement example of Fig. 2 is used.

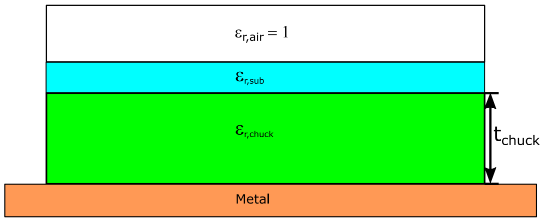

Fig. 1. Multilayered measurement setup.

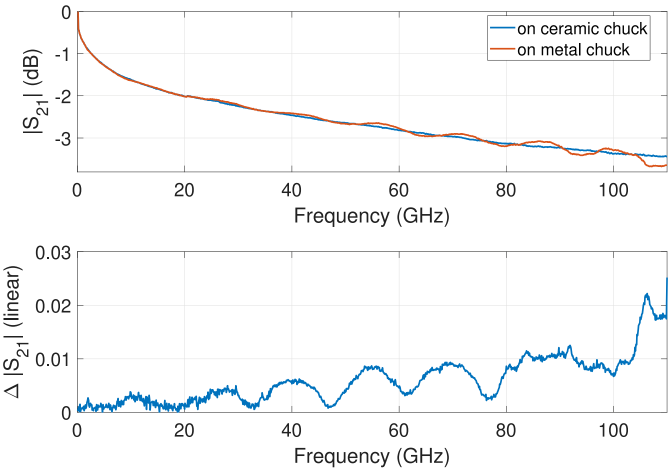

Fig. 2. Measurement of a CPW with l = 5400 µm on fused silica substrate using different chucks: Transmission coefficient $|S_{21}|$ and complex difference $\Delta|S_{21}|$ between the transmission on metal and ceramic chuck.

Fig. 2 shows the measured transmission coefficient $|S_{21}|$ and the complex difference $\Delta|S_{21}|$ between the transmission on metal and ceramic chuck for a CPW with length of l = 5400 µm on a fused silica substrate ($\epsilon_{\text{r,sub}}$ = 3.78) according to the following definition, using the ceramic chuck measurement as reference:

$$\Delta|S_{21}| = |S_{21,DUT} - S_{21,ref}| \tag{1}$$

All the measurements were performed with GGB probes with a 100 µm pitch. The measured data were processed with a mTRL calibration according to [8]. The defining parameters of the CPW cross section are the signal width w = 62 µm, the gap width s = 6 µm, the metal ground width w_g = 250 µm, the metal thickness t = 0.534 µm, and the thickness h = 254 µm

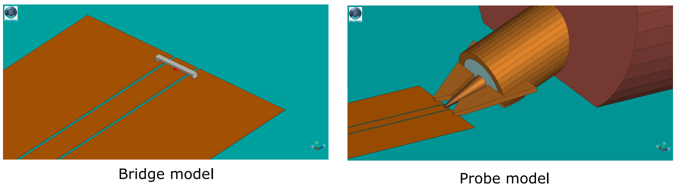

Fig. 3. Excitation models used in the em simulation.

of the fused silica substrate with a relative permittivity of $\epsilon_r = 3.78$. This substrate was also used in [9].

Fig. 2 clearly demonstrates that in the metal chuck case peculiarities and strong ripples are present in the transmission coefficient S_{21} and in the complex difference $\Delta|S_{21}|$. The ceramic chuck curve on the other hand shows a smooth behavior within the investigated frequency range. The thickness of the ceramic chuck used in the measurements is t_{chuck} = 8000 µm which represents an almost ideal condition. In some applications thinner chuck materials have to be used because of e.g. thermal considerations. With this motivation, a systematic study of the chuck conditions via em simulations will be presented in the next sections.

II. Systematic Study of Chuck Conditions

In order to simplify the investigation, a single DUT without neighboring structures is used in the stackup of Fig. 1 together with a perfect electric conductor (PEC) as boundary condition for the metal chuck. For the excitation, two different models, the simplified bridge model and the probe model of Fig. 3 are employed. The simplified bridge model [10] makes use of a conducting bridge between the ground planes of the CPW structure with a lumped element excitation placed in the center of the signal conductor. The probe model describes the probe used for measurements with realistic dimensions and has been utilized already in several investigations [2], [1] and [11].

A. Case 1: $\epsilon_{r,sub} < \epsilon_{r,chuck}$

In Case 1 the permittivity of the substrate is lower than that of the ceramic chuck ($\epsilon_{\text{r,sub}} = 3.78 < \epsilon_{\text{r,chuck}} = 6.5$), which is in compliance with the recommendation of the guide [7]. The CPW dimensions of the measured DUT (Fig. 2) are used and the ceramic chuck thickness is varied between 0 (direct measurement on metal chuck) and 8000 µm (measurement on ceramic chuck). The electromagnetic simulations were performed with CST from Dassault Systemes [12].

Fig. 4 shows the simulated electric fields for the CPW excited by the different models of Fig. 3 for different chuck thicknesses t_{chuck} = 0, 500, 2000 µm. At first sight, one can state that the parasitic effects for all the thicknesses are more pronounced when using probes for excitation. Secondly, the ceramic thickness determines the propagation path of the CPW mode.

For t_{chuck} = 0, a superposition of two modes, the CPW mode and the parallel plate line (PPL) mode, with different phase velocities can be observed. When using the bridge model for excitation, the PPL mode is only propagating along the CPW line and interacts with the CPW mode causing a phase distortion. On the other hand, when using the probe model for excitation, the propagation path of the PPL mode changes. The PPL mode is travelling to the probe needles and is transferred into the air region surrounded by the absorber enclosing the coaxial line of the probe. This in turn causes more pronounced effects in the environment of the DUT. With increasing t_{chuck} of 500 or 2000 µm the energy leaks into the ceramic chuck and is bounced back from the electric backside causing reflections coupling back into the DUT. This effect is also more pronounced for the probe excitation.

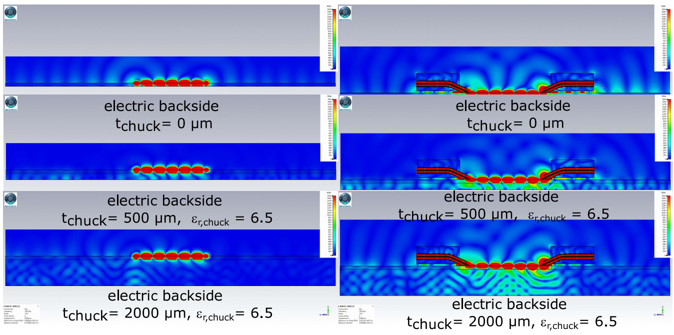

Fig. 4. Cross-sectional view of electric fields at f = 100 GHz of the CPW on fused silica excited by bridge (left) and probe model (right) for different ceramic chuck thicknesses t_{chuck}= 0, 500, 2000 µm and $\epsilon_{\text{r,chuck}}$= 6.5.

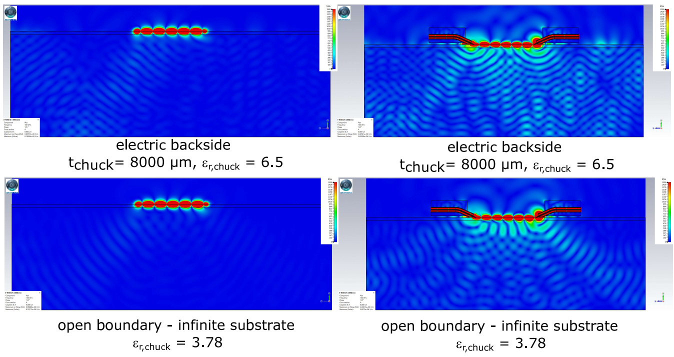

Fig. 5. Cross-sectional view of electric fields at f = 100 GHz of the CPW on fused silica excited by bridge (left) and probe model (right) for ceramic chuck thickness t_{chuck} = 8000 µm on metal backside and on open boundary.

Fig. 5 shows the comparison between t_{chuck} = 8000 µm and the ideal case with open boundary condition emulating an infinite substrate. The electric fields for t_{chuck} = 8000 µm are similar to the corresponding field patterns of the infinite substrate for both excitations. As expected, for the infinite substrate the energy is mainly radiated into the substrate with no reflections from the backside. For the CPW with finite chuck thickness t_{chuck} = 8000 µm only a small portion of the fields is reflected back from the electric backside.

Fig. 6 shows the corresponding complex difference ΔS_{21} of the CPW on fused silica substrate ($\epsilon_{\text{r,sub}}$ = 3.78) according to eq. (1) using the simulations of the infinite substrate as reference for subtraction. For t_{chuck} = 8000 µm the complex difference ΔS_{21} remains below 0.015 within the investigated frequency range for both excitations. Thus, the CPW case with t_{chuck} = 8000 µm on electric backside represents a good approximation of the infinite substrate.

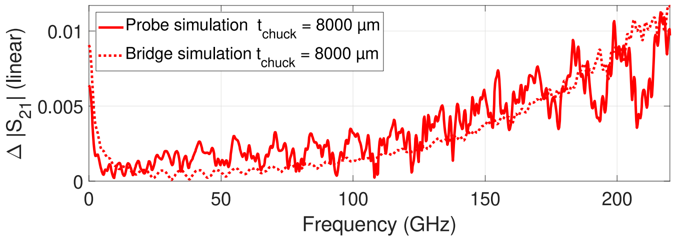

Fig. 6. Complex difference ΔS_{21} of the CPW on fused silica substrate ($\epsilon_{\text{r,sub}}$ = 3.78) and t_{chuck} = 8000 µm excited by different models.

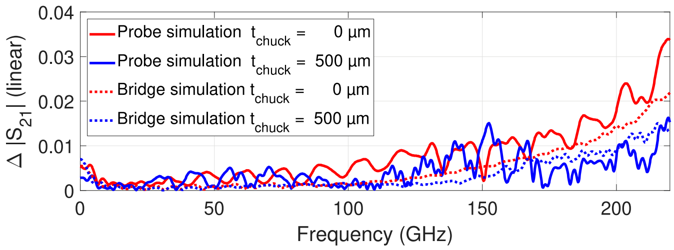

Fig. 7. Complex difference ΔS_{21} of the CPW on fused silica substrate ($\epsilon_{\text{r,sub}}$ = 3.78) for t_{chuck} = 0 and 500 µm excited by different models.

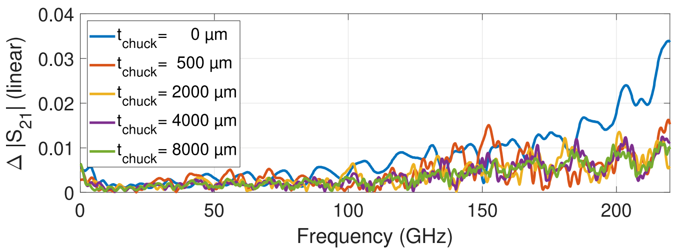

Fig. 8. Complex difference ΔS_{21} of the CPW on fused silica substrate ($\epsilon_{\text{r,sub}}$ = 3.78) for varied t_{chuck} between 0 and 8000 µm.

Fig. 7 plots the complex difference ΔS_{21} of the CPW for t_{chuck} = 0 and 500 µm using the simulations of the infinite substrate as reference. Compared to the bridge model, the deviation ΔS_{21} using probes for excitation is much higher. The strong reflections of the electric fields which couple back to the DUT (see Fig. 4) document themselves in maximum deviations of 0.04 at 220 GHz. Thus, we can conclude that the bridge model only includes the interaction of the CPW mode with the PPL mode and is therefore too ideal to reproduce the real measurement effects.

The results in Fig. 8 demonstrate to what extent the complex difference ΔS_{21} can be improved with increasing ceramic thickness t_{chuck}. With t_{chuck} larger than 4000 µm a deviation below 0.01 can be obtained up to 220 GHz, which is minimal compared to the other cases. For the given configuration, this indicates the minimum ceramic chuck thickness one should use to avoid PPL mode propagation and parasitic effects caused by reflections from the electric backside.

B. Case 2: $\epsilon_{r,sub} > \epsilon_{r,chuck}$

So far, Case 1 where the PlanarCal guideline has been fulfilled has been investigated. The question arises how the properties of the ceramic chuck would affect the S-parameters of the DUT if the PlanarCal guideline is violated. To this end, high-resistivity silicon (HRSi) is used as substrate material with a permittivity of $\epsilon_{\text{r,sub}} = 11.8 > \epsilon_{\text{r,chuck}} = 6.5$. This type of configuration is supposed to support the propagation of surface waves inside the substrate with the higher permittivity [11]. The CPW parameters are w = 11 µm, s = 8 µm, w_g = 54 µm, t = 0.525 µm and h = 400 µm in order to obtain a characteristic impedance close to 50 Ω. Again, simulations for different t_{chuck} values between 0 and 8000 µm were performed.

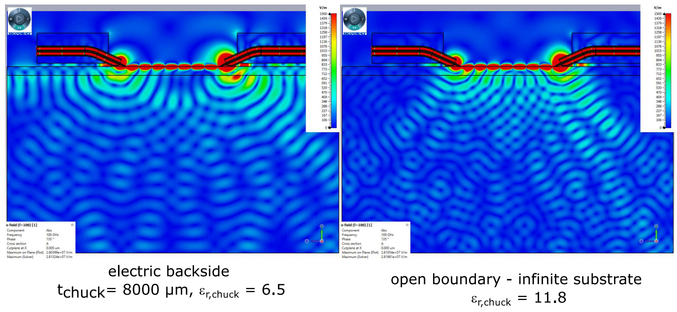

Fig. 9. Cross-sectional view of electric fields at f = 100 GHz of the CPW on HRSi substrate excited by probe model for ceramic thickness t_{chuck} = 8000 µm on electric backside and on open boundary condition.

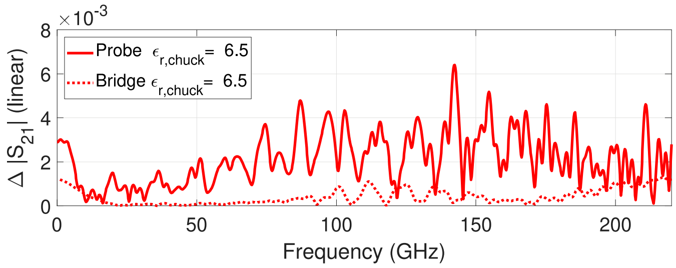

Fig. 10. Complex difference ΔS_{21} of the CPW on HRSi substrate over ceramic chuck with t_{chuck} = 8000 µm and different excitations.

Fig. 9 shows that the propagation of surface waves is indeed supported for t_{chuck} = 8000 µm on electric backside (left image). The electric fields of the surface wave are concentrated inside the HRSi substrate and spread over the whole substrate. The surface wave travels laterally away from the CPW with circular characteristics. Thus, the field patterns differ from that of the infinite substrate case where the energy mainly leaks and is radiated into the substrate (Fig. 9, right image). The different field patterns lead to a maximum ΔS_{21} of around 0.007 for the probe and 0.0015 for the bridge excitation using the simulations of the infinite substrate as reference (Fig. 10). Again, the bridge model is too ideal to describe the measurement effects seen with realistic probe models.

The field plots in Fig. 11 confirm the above statements. For t_{chuck} = 500 µm there is a superposition of three different effects: a stronger probe coupling to the surface wave, the PPL mode and a reflection path of the PPL mode from the electric backside. With increasing t_{chuck} the complex difference ΔS_{21} decreases (Fig. 12). Also here, one should keep t_{chuck} larger than 4000 µm to mitigate the propagation of the PPL mode and the parasitic effects caused by the reflections from the electric backside.

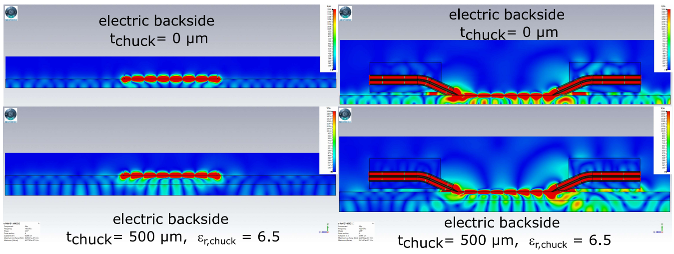

Fig. 11. Cross-sectional view of electric fields at $f = 100\,\text{GHz}$ of the CPW on HRSi substrate excited by bridge (left) and probe model (right) for ceramic thicknesses $t_{\text{chuck}} = 0$ and 500 µm.

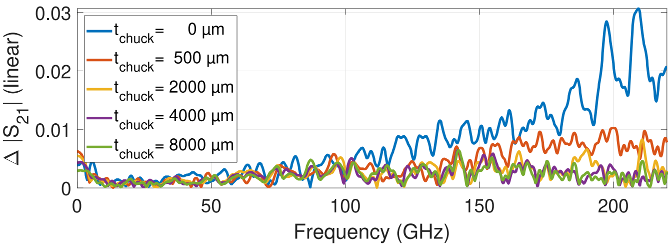

Fig. 12. Complex difference ΔS_{21} of the CPW on HRSi substrate for t_{chuck} varied between 0 and 8000 µm.

III. Discussion of Results

Analyzing the above results, one can state that it is absolutely necessary to apply realistic probe models to describe effects occurring in real measurements. It has been shown that a ceramic chuck with $t_{\text{chuck}} = 8000$ µm represents a good approximation for the infinite substrate. A ceramic chuck thickness of at least $t_{\text{chuck}} = 4000$ µm helps to mitigate the effect of PPL mode for both cases $\epsilon_{\text{r,sub}} < \epsilon_{\text{r,chuck}}$ (in compliance with the PlanarCal guide) and $\epsilon_{\text{r,sub}} > \epsilon_{\text{r,chuck}}$ (violation of the PlanarCal guide).

For $\epsilon_{\text{r,sub}} > \epsilon_{\text{r,chuck}}$ additionally the surface wave can propagate which also affects the S-parameters of the DUT. Therefore, one should additionally consider that the configuration simulated in this investigation was simplified to a single DUT with ideal lateral boundary conditions. In reality, the DUT is surrounded by neighboring structures, and the lateral dimensions of the substrate are finite. Therefore, in real measurements the surface waves can travel laterally from the probe excitation and can be reflected at any discontinuities (such as e.g. neighboring structures or substrate edges) and are coupled back to the DUT. Further investigations show that this effect is more critical, underlining the importance of complying with the recommendation for $\epsilon_{\text{r,chuck}}$ stated in the PlanarCal guideline.

The ceramic thickness determines the influence of the PPL mode and its reflection from the backside, whereas the permittivity of the ceramic chuck affects the coupling to the surface waves. Currently, research is in progress for developing analytical expressions which will help to better predict the occurrence of surface waves in multilayered CB-CPW stackups.

IV. Conclusion

Summarizing the above results, one can state that both parameters of the ceramic chuck measurement boundary, i.e. thickness and permittivity, affect the measured S-parameters of the DUTs. Thus, the best way to improve the measurement results is to select a ceramic chuck with a permittivity larger or similar to that of the substrate containing the DUTs, which is in compliance with the PlanarCal guideline [7]. Additionally, a ceramic thickness larger than 4 mm should be chosen to mitigate the effect of the PPL mode.

Acknowledgment

The authors acknowledge support by the European Metrology Programme for Innovation and Research (EMPIR) Projects 14IND02 PlanarCal and 18SIB09 TEMMT. Both projects (14IND02 and 18SIB09) have received funding from the EMPIR programme co-financed by the Participating States and from the European Union's Horizon 2020 research and innovation programme.

References

[1] G. N. Phung, F. J. Schmückle, R. Doerner, B. Kähne, T. Fritzsch, U. Arz, and W. Heinrich, "Influence of Microwave Probes on Calibrated On-Wafer Measurements," *IEEE Transactions on Microwave Theory and Techniques*, vol. 67, no. 5, pp. 1892–1900, 2019.

[2] F. J. Schmückle, T. Probst, U. Arz, G. N. Phung, R. Doerner, and W. Heinrich, "Mutual Interference in Calibration Line Configurations," in *2017 89th ARFTG Microwave Measurement Conference (ARFTG)*, 2017, pp. 1–4.

[3] M. Tsuji, H. Shigesawa, and A. A. Oliner, "New Surface-Wave-Like Mode on CPWs of Infinite Width and its Role in Explaining the Leakage Cancellation Effect," in *1992 IEEE MTT-S Microwave Symposium Digest*, 1992, pp. 495–498 vol.1.

[4] E. M. Godshalk, "Surface Wave Phenomenon in Wafer Probing Environments," in *40th ARFTG Conference Digest*, vol. 22, 1992, pp. 10–19.

[5] M. Spirito, C. De Martino, and L. Galatro, "On the Impact of Radiation Losses in TRL Calibrations," in *2018 91st ARFTG Microwave Measurement Conference (ARFTG)*, 2018, pp. 1–3.

[6] European Metrology Programme for Innovation and Research JRP Number 14IND02, "Microwave Measurements for Planar Circuits and Components." https://planarcal.ptb.de.

[7] M. Spirito, U. Arz, G. N. Phung, F. J. Schmückle, W. Heinrich, and R. Lozar, "Guidelines for the Design of Calibration Substrates, including the Suppression of Parasitic Modes for Frequencies up to and including 325 GHz," *EMPIR 14IND02 – PlanarCal, 2018, Physikalisch-Technische Bundesanstalt (PTB)*, 2018.

[8] R. B. Marks, "A Multiline Method of Network Analyzer Calibration," *IEEE Trans. on Microwave Theory and Techniques*, vol. 39, no. 7, pp. 1205–1215, 1991.

[9] U. Arz, K. Kuhlmann, T. Dziomba, G. Hechtfischer, G. N. Phung, F. J. Schmückle, and W. Heinrich, "Traceable Coplanar Waveguide Calibrations on Fused Silica Substrates up to 110 GHz," *IEEE Transactions on Microwave Theory and Techniques*, vol. 67, no. 6, pp. 2423–2432, 2019.

[10] T. K. Johansen, C. Jiang, D. Hadziabdic, and V. Krozer, "EM Simulation Accuracy Enhancement for Broadband Modeling of On-Wafer Passive Components," in *2007 European Microwave Conference*, 2007, pp. 1245–1248.

[11] G. N. Phung, F. J. Schmückle, R. Doerner, W. Heinrich, T. Probst, and U. Arz, "Impact of Substrate Modes on mTRL-Calibrated CPW Measurements in G Band," in *2018 48th European Microwave Conference (EuMC)*, 2018, pp. 194–197.

[12] "CST Studio Suite," 2020. [Online]. Available: https://www.3ds.com/products-services/simulia/products/cst-studio-suite/